Journal of Electroanalytical Chemistry 833 (2019) 63–69

Contents lists available at ScienceDirect

Journal of Electroanalytical Chemistry

journal homepage: www.elsevier.com/locate/jelechem

Carbon black/graphene-modified aluminum foil cathode current collectors for lithium ion batteries with enhanced electrochemical performances

Rubing Wang[a,b,1], Weiwei Li[a,c,*,1], Litian Liu[c], Yuting Qian[a], Fengkui Liu[a], Mingliang Chen[a], Yufen Guo[a,c], Liwei Liu[a,c,*]

[a] Key Laboratory of Nanodevices and Applications & Collaborative Innovation Center of Suzhou Nano Science and Technology, Suzhou Institute of Nano-Tech and Nano-Bionics, Chinese Academy of Sciences, 398 Ruoshui Road, Industrial Park, Suzhou 215123, PR China
[b] School of Nano Technology and Nano Bionics, University of Science and Technology of China, 96 Jinzhai Road, Baohe, Hefei 230026, PR China
[c] SZGraphene Nanotechnology Co., Ltd., 99 Jinji Lake Avenue, Industrial Park, Suzhou 215123, PR China

ARTICLE INFO

Keywords:
Graphene
Carbon black
Modified aluminum foil
Cathode current collector
Lithium-ion battery
Enhanced performances

ABSTRACT

Though aluminum foils are widely applied as cathode current collectors for lithium ion batteries, they still face many challenges, such as the limited contact area, weak adhesion with electrode materials and localized corrosion by electrolytes during long-term cycling, which will lead to the degradation of electrochemical performances. Here, graphene-modified aluminum foils and carbon black/graphene modified aluminum foils are prepared as the current collectors for lithium iron phosphate lithium ion batteries by a facile solution coating method. We find that the batteries fabricated with carbon black/graphene-modified aluminum foils exhibit largely improved electrochemical performances in rate capability, internal resistance and long-term cycling capacity retention, compared with the bare aluminum and graphene-modified aluminum foils. This work reveals the coatings of graphene nanosheets not only can increase the contact area and enhance the adhesion between electrode materials and current collectors, which is beneficial for their electrical contact and charge transport, but also can suppress the aluminum foil corrosion during long-term cycling. Meanwhile, the excessive coverage of graphene nanosheets will lower the battery performances due to the interlayer contact increment of graphene nanosheets. In addition, carbon black combines graphene to form a co-conductive network effectively compensating the low interlayer electrical conductivity of graphene nanosheets.

1. Introduction

With the development of modern consumer electronics and new energy vehicle industry, lithium-ion batteries (LIBs) have been put forward higher performance requirements, such as higher capacity and rate capability, more safety and longer life [1,2]. Current collectors as essential parts of LIBs, used to load electrode materials, collect the current from electrode materials and accomplish external output of large current, play an important role in electrochemical properties of LIBs [3]. Aluminum (Al) foil has been the most widely used cathode current collector for positive electrode materials due to its high conductivity, electrochemical and chemical stability and low cost [4]. However, Al foil current collectors still face a variety of challenges. The limited contact area and weak adhesion between electrode materials and current collectors will lead to the increased interface contact resistance, and further the internal resistance of LIBs. What's more, the localized corrosion of Al foils during long-time cycling is also a serious problem, causing the increase of resistance, detachment of electrode materials, microshort-circuits induced by resultant Al fragments and so on [4–6]. All of these factors will further result in deterioration of specific capacity, rate capability, safety and cycle stability of LIBs.

In order to improve the contact area and adhesion between electrode materials and current collectors, Al foil surface treatments are extensively applied to increase the surface roughness by chemical and electrochemical etching methods [7]. These processes bringing about larger contact area and stronger adhesion, in some degree, reduce the internal resistance, enhance the rate capability and extend the cycling life, but there exist the issues of anodic corrosion and decreased mechanical strength of Al foils as cathode current collectors.

Meanwhile, some methods on regulating the compositions of

* Corresponding authors at: Key Laboratory of Nanodevices and Applications & Collaborative Innovation Center of Suzhou Nano Science and Technology, Suzhou Institute of Nano-Tech and Nano-Bionics, Chinese Academy of Sciences, 398 Ruoshui Road, Industrial Park, Suzhou 215123, PR China.
E-mail addresses: wwli2009@sinano.ac.cn (W. Li), lwliu2007@sinano.ac.cn (L. Liu).
[1] These authors contributed equally to this work.

https://doi.org/10.1016/j.jelechem.2018.11.007
Received 10 July 2018; Received in revised form 3 October 2018; Accepted 5 November 2018
Available online 07 November 2018
1572-6657/

electrolytes have been reported to inhibit the corrosion of Al foil current collectors. $LiPF_6$-based electrolyte was proved to form AlF_3 passive layer on the natural Al_2O_3 layer at the surface of Al foil during the early cycles, which can protect the Al foil from corrosion [8–10]. But the both natural oxide layer and passive layer are too thin to resist corrosion at the long duration of cycling [11,12]. Superconcentrated imide electrolytes were found good candidates to suppress the formation and dissolution Al-complexes because of the largely decreasing solvent molecules or free anions in electrolytes foil corrosion through, and consequently realize the corrosion control [13,14]. However, such approach involved in high technical requirements, expensive cost and most importantly, sacrifice of lithium ion (Li^+) conductivity is still limited [15,16].

Recent years, carbon-coated Al foils have been widely applied to the popular commercial cathode current collectors [7,17]. This is because the existence of conductive carbon cover layer not only increases the contact area between electrode materials and Al foil but also as a buffer layer strengthens their adhesion, which effectively lowers the resistance and suppresses the resistance increase during charge-discharge process [18]. Besides, it also can prevent the corrosion of Al foil and improve the comprehensive performances of LIBs, such as the higher rate charge-discharge performance, better safety, as well as longer cycling life. The mainstream carbon coating materials in industry are low cost carbon black (CB) and graphite. Nevertheless, their thick coatings (2 to 5 μm) occupy too much weight and volume of electrodes, which compromises a large part of specific capacity and energy density.

Afterwards, the rising graphene with large specific surface area, high conductivity and light weight is applied to serve as the ideal carbon coat material. With less thickness (0.2 to 2 μm), stronger adhesion and higher conductivity, graphene has greater advantages in performance enhancement of LIBs than traditional CB and graphite. However, the nanostructure of graphene and carbon nanotube puts forward the technical problems in the dispersity of coating slurries and uniformity of coating.

Latest work about plasma enhanced chemical vapor deposition (PECVD) graphene-armored Al foil with enhanced anticorrosion performance as current collectors for LIBs has been reported and shown superior electrochemical performances, including longer cycling life, better rate performance and ameliorated self-discharging property [19]. Nevertheless, due to the low melting point of Al about 667 °C and high decomposition temperature of methane (CH_4) about 800 °C, PECVD is necessary to grow graphene on Al foils, which demands equipment and growth conditions strictly and is hard to achieve in somewhere else. In contrast, reduced graphene oxide (RGO) is technically mature in production, dispersion and accessible to large scale preparation.

Here we prepare graphene-modified Al foils (G-Al) as cathode current collectors for lithium iron phosphate ($LiFePO_4$, LFP) LIBs. The process is a facile solution coating through dip coating of graphene oxide (GO) aqueous solution on commercial Al foil, followed by a thermal reduction process. The LFP LIBs using G-Al with partial coverage of graphene (PG-Al) are found with enhanced electrochemical performances compared to those of bare Al and G-Al with full coverage of graphene (FG-Al), such as lower internal resistance, higher specific capacity, rate capability as well as cycling capacity retention. It can be attributed to the existence of graphene buffer layers on Al foils, the adhesion of LFP electrode materials and G-Al is effectively strengthened, and then the electrical contact and charge transport between them are improved [18]. Meanwhile, scanning electron microscope (SEM) shows the surfaces of current collectors with graphene coverage more intact and less corrosion than that of bare Al after 500 cycles, revealing the graphene nanosheets play an important role in protecting the Al from corrosion in the long-term cycling [19]. In addition, considering the low interlayer electrical conductivity of graphene, CB is introduced to obtain carbon black/graphene-modified Al foils (CB/G-Al). In result, the LFP LIBs fabricated with CB/G-Al exhibit further improved electrochemical performances over that with only graphene-covered Al foils. The LIBs based on PG-Al and CB/G-Al have pretty high specific capacities of 168.8 mAh g^{-1} and 169.9 mAh g^{-1} at the low rate charge-discharge process of 0.2 C, much higher than that of Al (147.7 mAh g^{-1}) and close to the theoretical capacity of 170 mAh g^{-1} [20]. After 500 cycles at the rate of 1 C, the specific capacity of LIB fabricated with CB/G-Al maintains 153.97 mAh g^{-1} with the capacity retention ratio of 94.8% higher than that with PG-Al of 120.5 mAh g^{-1} with the capacity retention ratio of 91.3%, and much higher than that with bare Al of 73.37 mAh g^{-1} with the capacity retention ratio of 57.3%.

2. Experimental section

2.1. Synthesis of GO

GO was prepared by a modified Hummers method similar to previous work [21,22]. Natural graphite power (3 g, 300 mesh, Alfa Aesar), Potassium persulfate (2.5 g, $K_2S_2O_8$, 99.0%, Alfa Aesar) and phosphorus pentoxide (2.5 g, P_2O_5, extra pure, Alfa Aesar) were added into concentrated sulfuric acid (14 ml, H_2SO_4, 95–98%, Sinopharm). The mixture was kept in an oil bath of 80 °C for 6 h. After cooled down to room temperature, the mixture was diluted by 500 ml deionized water, filtered and washed by large amount of deionized water to remove the residual acid until the pH value of the rinse water became neutral. The product was dried under ambient condition for 3 days to obtain the pre-oxidize graphite powder applied to further oxidation by Hummers' method. The pre-oxidize graphite powder was put into 120 ml concentrated H_2SO_4 in an ice bath of 0 °C, and then under vigorous stirring, potassium permanganate (15 g, $KMnO_4$, ≥99.5%, Sinopharm) was added gradually. The mixture was kept stirring in a water bath of 35 °C for 2 h. Afterwards, 1000 ml deionized water and 20 ml hydrogen peroxide (H_2O_2, 30%, ≥30%, Sinopharm) were added to terminate the reaction. The mixture was filtered and washed with 10% hydrochloric acid (HCl, 36–38%, Sinopharm) to remove metal ions. The resultant was centrifuged and washed to a neutral pH, and then dispersed in deionized water by ultrasound at 100 W for 30 min. GO powder was finally obtained by freeze-drying the GO dispersion.

2.2. Preparation of G-Al, CB/G-Al and CB-covered Al (CB-Al) foil current collectors

GO aqueous solutions were prepared by ultrasonic progress of certain amount GO powder in deionized water for 30 min under 100 W. Al foils were immersed into specific GO solution, and then taken out and put into the oven with 80 °C for 10 min to obtain dry GO-covered Al (GO-Al) foils. Afterwards, GO-Al foils were annealed at 200 °C under N_2 (50 sccm) and H_2 (50 sccm) mixed atmosphere for 1 h to obtain G-Al foils. GO solutions with concentration of 0.05, 0.25, 1 and 5 mg/ml were used to prepare G-Al-0.05, PG-Al corresponding to G-Al-0.25, G-Al-1 and FG-Al corresponding to G-Al-5, respectively.

CB aqueous dispersion was prepared by ultrasonic progress of CB and dispersant agents (content equal to 1% of CB) in deionized water. CB dispersions with concentration of 0.05, 0.25 and 5 mg/ml were used to prepare CB-Al-0.05, CB-Al-0.25 and CB-Al-5, respectively.

CB/GO aqueous dispersions were prepared through ultrasonic mixture of GO solution and CB aqueous dispersion. Similarly, CB/GO-covered Al (CB/GO-Al) and CB/G-Al foils were prepared in the same method as mentioned above. The GO concentration kept 0.1 mg/ml. Several types of CB/G-Al were obtained by coating dispersions with CB/GO ratios 1/4, 1 and 4, corresponding to CB/G-Al-1/4, CB/G-Al-1 and CB/G-Al-4, respectively.

2.3. Fabrication of LIBs

LFP powder (M12, Aleees), CB (Super P, Timcal) and polyvinylidene fluoride (PVDF, HSV900, Arkema) were mixed in *N*-methyl pyrrolidone

(NMP, ≥99.9%, MYJ Chemical) to prepare LFP electrode slurry (LFP:CB:PVDF = 80:10:10). The slurry was blade coated on Al, G-Al and CB/G-Al foils, and then dried in vacuum oven at 130 °C for 24 h to prepare LFP electrodes with different current collectors. The electrodes (circular shape with diameter of 13 mm, thickness of electrode materials about 20 μm after rolling, mass loading of electrode material about 1.7 ± 0.2 mg/cm^2) were fabricated into half cells with lithium metal electrodes (14.5 × 0.45, Shenzhen Mingruixiang), membrane (3501, Celgard), electrolyte (LD-134BJ, Dongguan Shanshan), and button cell modules (CR 2025, Shenzhen Mingruixiang).

2.4. Characterizations

The morphology of current collectors was observed using a scanning electron microscope (SEM, Quanta FEG 250, FEI). The Raman spectra were carried out by a Raman spectrometer (LabRam HR800-UV-NIR, λ = 532.15 nm, HORIBA Jobin Yvon). The X-ray photoelectron spectroscopy (XPS) spectra were measured by an X-ray photoelectron spectroscopy (ESCALAB 250 XI, Thermo Scientific). The electrical resistivity of electrodes was tested by a multifunction digital four-probe tester (ST 2258C, Jingge Electronics).

2.5. Electrochemical measurements

An electrochemical workstation (CHI660D, CH Instruments) was carried on for the electrochemical impedance spectroscopy (EIS) tests. The EIS analyses were tested at frequencies ranging from 0.01 Hz to 100 kHz with amplitude of 5 mV at open current potentials. The rate test and charge-discharge curves at 1 C were performed by a battery tester (CT-3008-5V50mA-S4, NEWARE).

3. Results and discussion

3.1. The typical morphology and structure of G-Al foils and electrochemical performances of the LIBs

Raman and XPS are employed to determine the structure and functional groups of GO before and after 200 °C thermal annealing, respectively. Fig. 1a illustrates the Raman spectra of GO-Al and G-Al. Each of the spectra has obvious D band (~1343 cm^{-1}) on behalf of disorder, defect or sp3 diamond band, and G band (~1599 cm^{-1}) related to sp2 graphite. What's more, there is a comparatively low 2D band (~2750 cm^{-1}) which is commonly seen in 2D graphene as an important feature to distinguish graphene from bulk graphite [23,24]. The appearance of 2D bands of both Raman spectra of GO-Al and G-Al means the existences of 2D GO and graphene. The intensity ratio ID/IG corresponds to the degree of disordering of graphene or GO. ID/IG of G-Al is lower than that of GO-Al, indicating that reduced GO has higher ordering and lower defeat, which can be attributed to removal of the oxygen-containing functional groups during the thermal reduction process. It also can be further proved by the XPS spectra before and after reduction. The C1s XPS spectra in Fig. 1c, d show that the proportion of oxygen-containing functional groups, such as C═O, C—OH, C—O—C and COOH, obviously decreases after 200 °C thermal reduction.

Several types of graphene-modified Al foils are made by dip coating GO dispersions with different concentrations (0.05, 0.25, 1 and 5 mg/ml) on Al foils, followed by 200°Cthermal annealing process, respectively. Fig. 2 shows their corresponding typical SEM images. When the concentration of GO dispersion is diluted to 0.05 mg/ml (G-Al-0.05), the coverage level of graphene on Al foils is low so that large area of bare Al is exposed (Fig. 2a). With the concentration of GO increasing to 0.25 mg/ml (G-Al-0.25), the graphene nanosheets uniformly distribute on the Al foil and still leave small regions of bare Al exposed (Fig. 2b), providing larger contact area for the electrode material than that of G-Al-0.25. When the concentration of GO increases beyond 0.25 mg/ml such as 1 mg/ml (G-Al-1) and 5 mg/ml (G-Al-5), respectively, the coverage levels of graphene on Al foils increase obviously and the graphene nanosheets are easily to overlap and form films which nearly fully cover Al foils (Fig. 2c, d). Based on the SEM results, the G-Al-0.05, G-Al-0.25 and G-Al-5 are performed as the graphene modified current collectors to investigate their LIB performances, respectively. The rate capacity and initial Nyquist plots are demonstrated in Figs. S1 and S2. As a result, G-Al-0.25 current collector shows the best LIB performances than those of G-Al-0.05 and G-Al-5, such as the rate capacity and internal resistance. It concludes that G-Al-0.25 has the optimal coverage level of graphene in our comparison experiments. Next, the PG-Al and FG-Al as current collectors corresponding to G-Al-0.25 and G-Al-5, respectively, are employed to further research their LIBs performance.

Half cells are assembled to investigate the electrochemical performances of the LFP LIBs with Al, PG-Al and FG-Al as current collectors. The charge-discharge curves, rate capability and cycle profiles in Fig. 3a–c reveal that LIBs of PG-Al possess the best electrochemical performances compared with those of Al and FG-Al. By contrast with the bare Al based LIBs, due to the large contact area for electrode materials caused by the existence of graphene buffer layer, the adhesion of the LFP electrode material and G-Al is effectively strengthened, and then the electrical contact and charge transport between them are largely improved, which is similar to other carbon materials [7]. It is worth noting that with the coverage of graphene nanosheets on Al foils increases from PG-Al to FG-Al, the performances of specific capacity, rate capability and cycling stability of LIBs turn worse. On one hand, for the case of FG-Al with graphene nanosheets stacking and fully covering Al foils, the charges have to transport cross the interlayer direction of graphene nanosheets to finish electrochemical process, but the low interlayer electrical conductivity of graphene nanosheets restricts the charge to transport between current collectors and electrode materials. On the other hand, for the case of PG-Al with proper graphene coverage on Al foils, lots of charges can fast transport between electrode materials and Al foils directly, and the graphene interlayer transport of charges is not dominating. Furthermore, it is confirmed by the EIS results in Fig. 3d. The Nyquist plot contains a semicircle in the high frequency region and an inclined line in the low frequency region, which represent the charge transfer resistance (R_{ct}) occurring at the electrode/electrolyte interface and Warburg impedance (W_o) related to Li^+ diffusion in the electrode, respectively [18]. Though the mediation of graphene has no distinct influence on diffusion in electrodes, LIBs of G-Al have lower R_{ct} than that of Al, because of the improved electrical contact of electrode materials and current collectors. While in regard to the LIBs of FG-Al, the R_{ct} is found larger than that of PG-Al. Although graphene nanosheets can improve the electrical contact of LFP electrodes and current collectors by increasing the adhesion of them, the low interlayer conductivity of graphene restricts the charge transport in the interlayer direction, which consists with the resistivity test results of electrodes with different as prepared current collectors. As shown in Fig. S3, obvious resistivity reduction of LFP electrodes with PG-Al can be observed, while FG-Al based electrodes show even larger resistivity than that of Al.

Cycling stability is an important performance index of LIBs determining their lifetime. During long term cycling demonstrated in Fig. 3c, the LFP LIBs of PG-Al and FG-Al (LFP/PG-Al, LFP/FG-Al) maintain higher specific capacities (91.3% and 83.8% of initial capacities after 500 cycles) than LFP LIB with Al (LFP/Al), whose specific capacity fades rapidly to 57.3%. Meantime, the coulombic efficiency of all the LIBs is kept close to 100% without drop in Fig. S4. The Nyquist plots after cycling test in Fig. S5 also coincides with the capacity retention results. It can be obviously observed that the EIS degradations of LFP/PG-Al and LFP/FG-Al are much slighter than that of LFP/Al after long-time cycling. To investigate reason for the higher cycling stability of LFP/PG-Al and LFP/FG-Al than LFP/Al, the coin cells after cycling test are taken apart. SEM images of current collectors after cycling are shown in Fig. 4. As shown in Fig. 4a, there are many obvious holes and Al fragments on the surface of bare Al foil current collector due to the

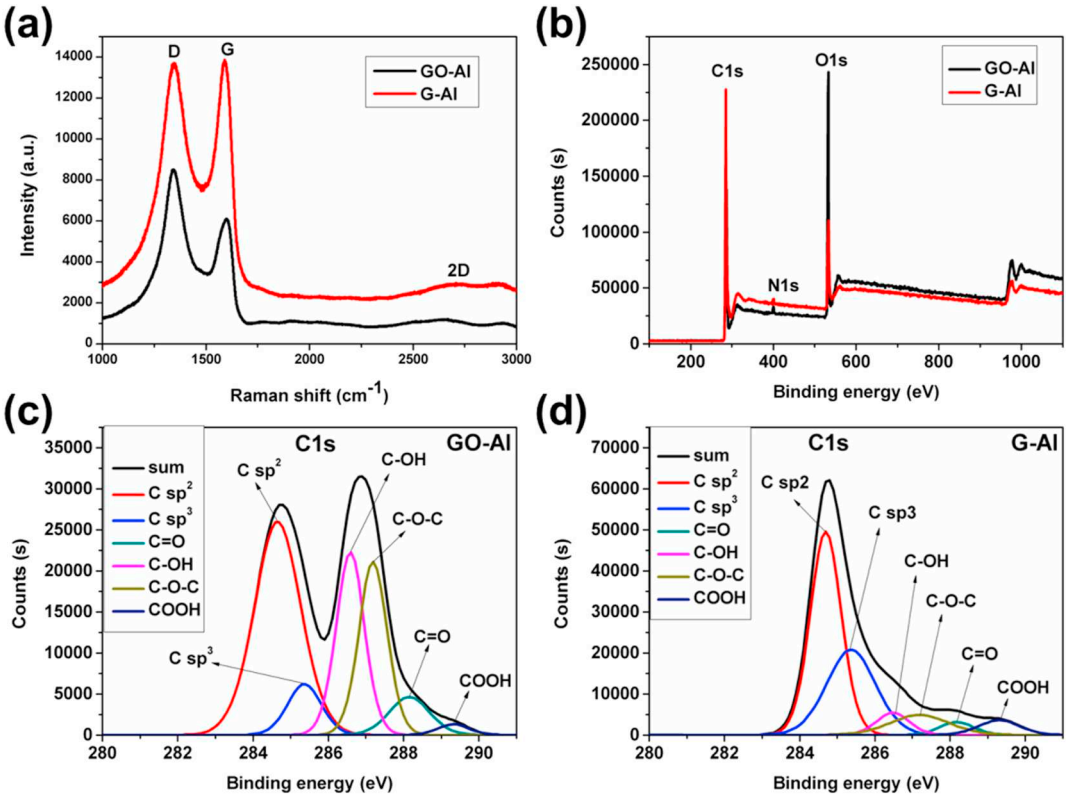

Fig. 1. (a) The Raman spectra of GO before and after thermal annealing on Al foil. (b) The XPS spectra of GO before and after thermal annealing on Al foil. (c) The C1s XPS spectra of GO on Al foil. (d) The C1s XPS spectra of GO after thermal annealing on Al foil. The concentration of GO dispersion is 5 mg/ml.

heavy corrosion during the cycling process causing the increase of resistance, detachment of electrode materials, microshort-circuits and so on. While the surface structures of PG-Al and FG-Al in Fig. 4b and c, respectively, keep relatively intact, suggesting their excellent anti-corrosion performance. Therefore, it can be concluded that graphene nanosheets play an important role in protecting the Al foil from corrosion by electrolyte during long term cycling, which is helpful for the cycling stability and safety of LIBs. However, besides the low interlayer electrical conductivity of graphene, exceeding graphene will form loose structure on the surface of Al during long term cycling, as shown in Fig. 4c, which will weaken the electrical contact between electrode material and current collector and further lead to capacity degradation.

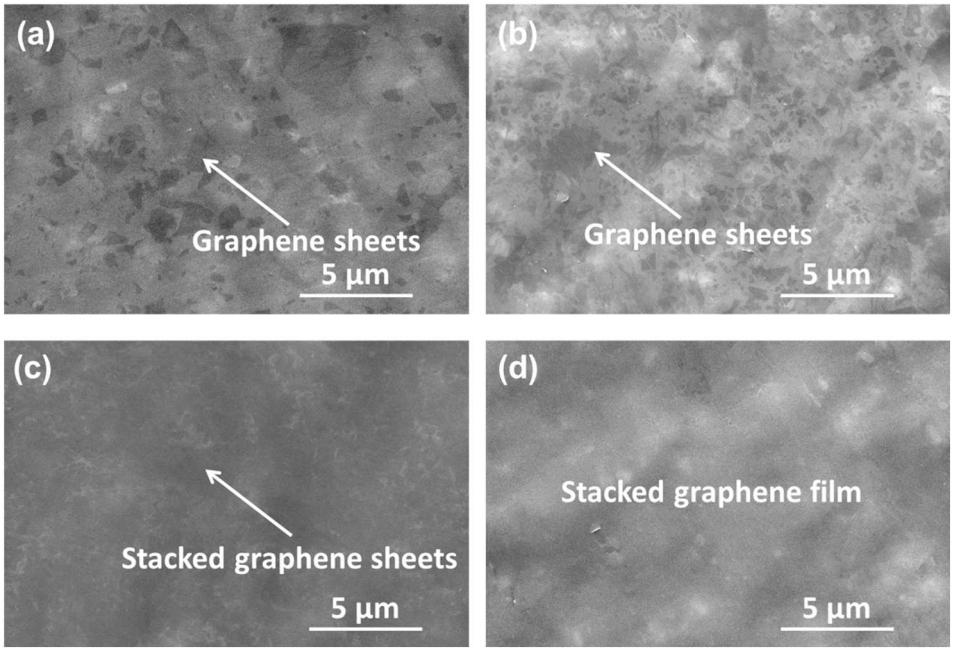

Fig. 2. The typical SEM images (×20 K) of (a) G-Al-0.05, (b) G-Al-0.25, (c) G-Al-1 and (d) G-Al-5 foils.

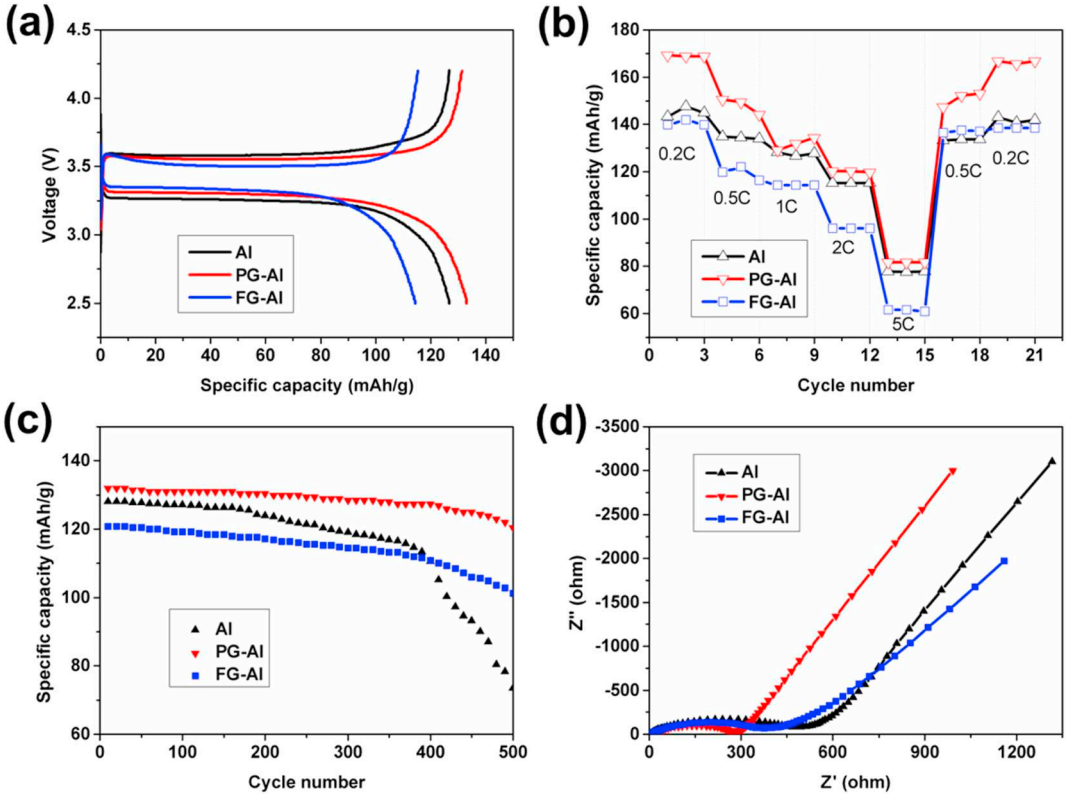

Fig. 3. The electrochemical performances of LFP LIBs with Al, PG-Al and FG-Al current collectors. (a) The charge-discharge curves at the rate of 1 C. (b) The rate performances. (c) The long-term cycling stability at the rate of 1 C. (d) The initial Nyquist plots before charge-discharge test.

3.2. The electrochemical performances of LIBs based on CB-Al and CB/G-Al

CB, another carbon nanoparticle, is a good candidate as the coating material of the current collector for its properties of chemical-resistance, high isotropic electronic conductivity, light weight and low cost. Therefore, the LIB performances of CB-Al-5, CB-Al-0.25 and CB-Al-0.05 foils with different CB coverage degrees corresponding to the concentration of CB of 5 mg/ml, 0.25 mg/ml and 0.05 mg/ml, respectively, are studied. The typical SEM images in Fig. S6 show that CB-Al-5 has CB aggregations on the surface of Al foil, while CB-Al-0.25 and CB-Al-0.05 have relatively uniform CB dispersion. CB-Al-0.25 and CB-Al-0.05 are found with enhanced electrochemical performances compared to those of CB-Al-5, such as lower internal resistance, higher specific capacity, rate capability as well as cycling capacity retention in Figs. S7–9. Both CB distribution and LIB performances suggest the appropriate concentration range of CB is 0.05–0.25 mg/ml.

To improve the electrochemical performances of G-Al or CB-Al based LIBs further. CB/G composites are employed as the co-conductive agents to compensate the low interlayer electrical conductivity of graphene by forming a 3D effective conductive network on Al foils. Due to the appropriate coverage level of G-Al and CB-Al demonstrated above, the GO concentrations are kept 0.1 mg/ml, and CB/G-Al-1/4, CB/G-Al-1 and CB/G-Al-4 are prepared by coating CB/GO dispersions with CB/GO concentration ratios of 1/4, 1 and 4, respectively. The corresponding SEM images in Fig. S10 show CB/G-Al-1/4 and CB/G-Al-1 have graphene and CB uniformly disperse on Al, while CB/G-Al-4 has graphene and CB aggregations obviously, indicating that with the increase of CB ratio, the composites tend to aggregate. The rate performance of CB/G-Al-1 in Fig. S11 exhibits much higher specific capacity at high rate of 5 C than those of CB/G-Al-1/4 and CB/G-Al-4, revealing its superior rate performance. Meantime, the Nyquist plots before charge-discharge cycles shown in Fig. S12, suggests the CB/G-Al-1 has lower Rct than those of CB/G-Al-1/4 and CB/G-Al-4, which is consist with the rate performance results. The LIB performances show the rule of CB/G-Al-1 > CB/G-Al-1/4 > CB/G-Al-4. The existence of graphene in some extent can help CB adhere on Al. Moderate addition of CB can further increase electrical contact between the electrode material and current collector. However, exceeding CB will increase aggregations and form loose carbon coverage between electrode material and current collector, turning against the electrical contact and charge

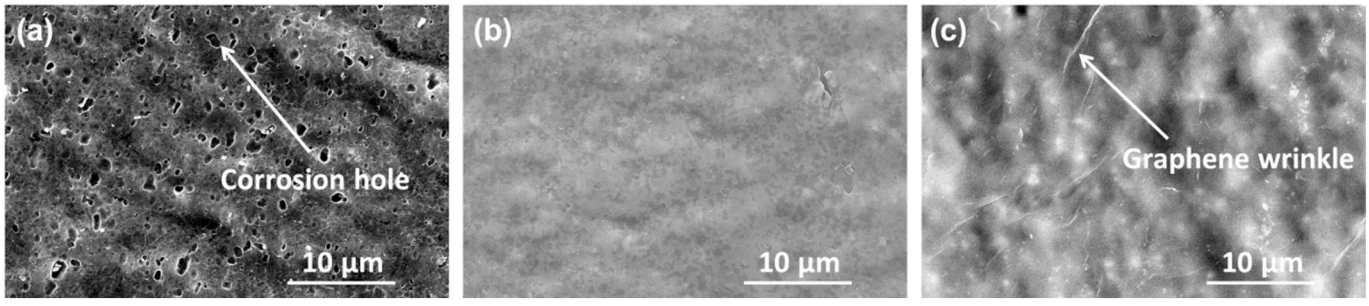

Fig. 4. The typical SEM images (×10 K) of the (a) Al, (b) PG-Al and (c) FG-Al current collectors after 500 cycles.

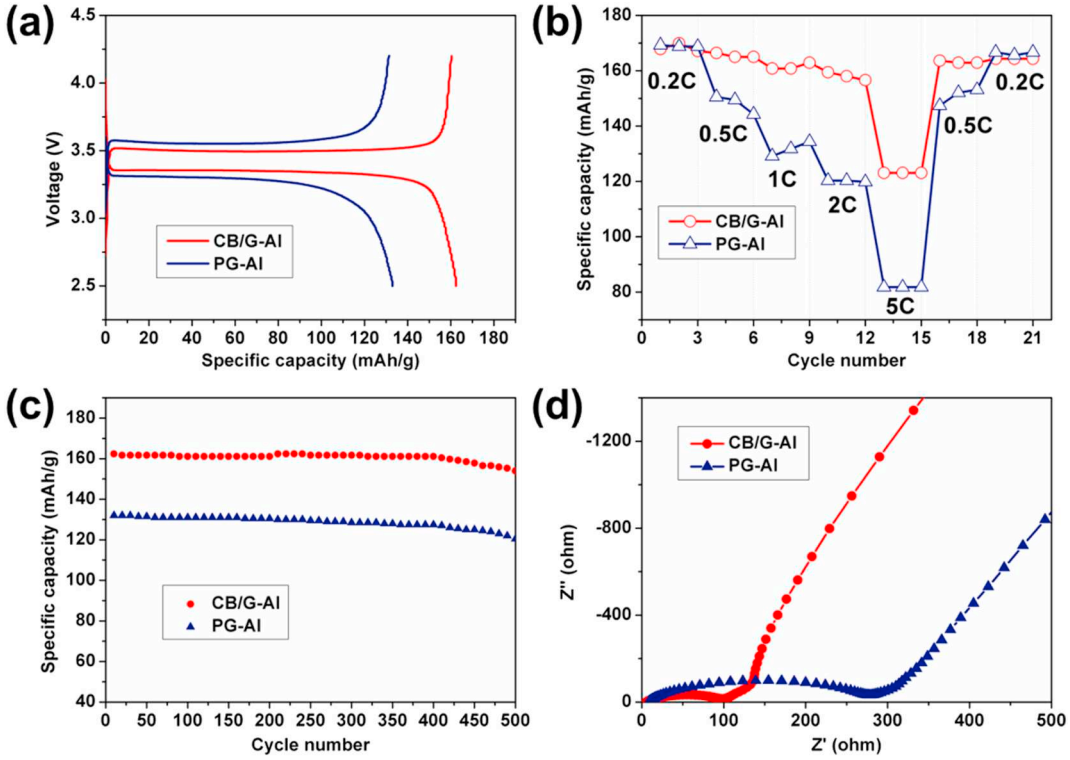

Fig. 5. The electrochemical performances of LFP LIBs with CB/G-Al and PG-Al. (a) The charge-discharge curves at the rate of 1 C. (b) The rate performances. (c) The long-term cycling stability at the rate of 1 C. (d) The initial Nyquist plots before charge-discharge test.

transfer. Meanwhile, CB/G-Al-1 mentioned below corresponding to CB/G-Al is used to compare with PG-Al to further investigate the improvement of LIB performances due to the addition of CB.

Fig. 5a shows the charge-discharge curves of LFP LIBs with CB/G-Al compared with PG-Al. The polarization between the charging and discharging plateaus for the LFP LIB with CB/G-Al foil (LFP/CB/G-Al) is 0.14 V at the rate of 1 C lower than that of LFP LIB with PG-Al foil (LFP/PG-Al) of 0.25 V, which illustrates the addition of CB makes the polarization of LFP/CB/G-Al much smaller than that of LFP/PG-Al. It can be attributed to the lower internal resistance of LFP/CB/G-Al. Correspondingly, the resistivity of CB/G-Al electrodes decreases an order of magnitude compared with those of Al and G-Al, as demonstrated in Fig. S13. In addition, the rate performances of LFP/CB/G-Al and LFP/PG-Al are shown in Fig. 5b. LFP/CB/G-Al exhibit much higher specific capacities at higher rates (e.g. at a rate of 5 C), revealing superior rate performance. After 500 cycles at the rate of 1 C, the specific capacity of LFP/CB/G-Al maintain 153.97 mAh g^{-1} with the capacity retention ratio of 94.8% higher than that with PG-Al of 120.5 mAh g^{-1} with the capacity retention ratio of 91.3%, and much higher than that with bare Al of 73.37 mAh g^{-1} with the capacity retention ratio of 57.3%, suggesting the good cycling performance. Meantime, the coulombic efficiency in Fig. S14 maintains close to 100% without any drop. The Nyquist plots before and after 500 charge-discharge cycles at the rate of 1C are shown in Figs. 5d and S15, respectively, suggesting the LFP/CB/G-Al has lower R_{ct} than that of LFP/PG-Al, which is consist with the rate performance results. Such superior performances can be attributed to the following points. On one hand the addition of CB further improves the adhesion between electrode materials and current collectors. On the other hand, CB combines graphene to form a co-conductive network, which can effectively compensate the disadvantage of poor interlayer conductivity of graphene.

4. Conclusions

In summary, we facilely prepare the G-Al and CB/G-Al foils as current collectors for LFP LIBs through dip coating of the GO solutions or CB/GO dispersions on Al foils and followed by a heat treatment. Compared with Al, the LIBs fabricated with certain PG-Al and CB/G-Al exhibit obvious enhanced electrochemical performances in internal resistance, specific capacity, rate performance and cycling stability. These results are attributed to the effect of graphene nanosheets and CB as follows: On one hand, the existence of graphene buffer layers on Al foils increases the contact area and enhance the adhesion between electrode materials and current collectors effectively, resulting in their improved electrical contact and charge transport. On the other hand, the layer-like structure of graphene nanosheets on the surface of Al foil effectively suppresses the electrolyte corrosion of current collectors during the long-term cycling process. Meanwhile, appropriate coverage level of graphene is considerable because the excessive coverage of graphene nanosheets on the Al foil surface will lower the LIB performances attributed to the interlayer conductivity reduction of excessive graphene nanosheets of layer contact increment. The last but not the least, the addition of CB on the current collectors, forming a co-conductive network with graphene, compensates the low interlayer electrical conductivity of graphene nanosheets and facilitates the charge transport, bringing about further preferable electrochemical performances. This work develops a facile method to prepare graphene-modified Al foils, which acts as the novel current collectors with lighter and thinner coatings for higher performances and safe LIBs, as well as other energy-storage devices.

Acknowledgment

This work was supported by the National Natural Science Foundation of China [Grant Nos. 11474310 and 61605237], the State Key Program of National Natural Science Foundation of China [Grant No. 61734008], the External Cooperation Program of BIC, Chinese Academy of Sciences (Grant No. 121E32KYSB20160071) and the projects of Jiangsu Province and Suzhou City [Grant Nos. BE2016006-3, BK20150366, BK20150367 and SYG201629]. The authors are also

grateful for the technical support of Nano-X, the Platforms of Characterization & Test, Collaborative Innovation Center of Suzhou Nano Science and Technology, and Nanofabrication Facility from Suzhou Institute of Nano-Tech and Nano-Bionics.

Declarations of interest

None.

Appendix A. Supplementary data

Supplementary data to this article can be found online at https://doi.org/10.1016/j.jelechem.2018.11.007.

References

[1] G. Kucinskis, G. Bajars, J. Kleperis, Graphene in lithium ion battery cathode materials: a review, J. Power Sources 240 (2013) 66–79.
[2] J.B. Goodenough, Evolution of strategies for modern rechargeable batteries, Acc. Chem. Res. 46 (2013) 1053–1061.
[3] J.B. Goodenough, K.S. Park, The Li-ion rechargeable battery: a perspective, J. Am. Chem. Soc. 135 (2013) 1167–1176.
[4] S.T. Myung, Y. Hitoshi, Y.K. Sun, Electrochemical behavior and passivation of current collectors in lithium-ion batteries, J. Mater. Chem. 21 (2011) 9891–9911.
[5] F. Li, Y. Gong, G. Jia, Q. Wang, Z. Peng, W. Fan, B. Bai, A novel dual-salts of LiTFSI and LiODFB in $LiFePO_4$-based batteries for suppressing aluminum corrosion and improving cycling stability, J. Power Sources 295 (2015) 47–54.
[6] S.S. Zhang, T.R. Jow, Aluminum corrosion in electrolyte of Li-ion battery, J. Power Sources 109 (2002) 458–464.
[7] H.C. Wu, H.C. Wu, E. Lee, N.L. Wu, High-temperature carbon-coated aluminum current collector for enhanced power performance of $LiFePO_4$ electrode of Li-ion batteries, Electrochem. Commun. 12 (2010) 488–491.
[8] K. Kanamura, T. Okagawa, Z.I. Takehara, Electrochemical oxidation of propylene carbonate (containing various salts) on aluminium electrodes, J. Power Sources 57 (1995) 119–123.
[9] M. Morita, T. Shibata, N. Yoshimoto, M. Ishikawa, Anodic behavior of aluminum in organic solutions with different electrolytic salts for lithium ion batteries, Electrochim. Acta 47 (2002) 2787–2793.
[10] X.Y. Zhang, T.M. Devine, Identity of passive film formed on aluminum in Li-ion battery electrolytes with $LiPF_6$, J. Electrochem. Soc. 153 (2006) B344–B351.
[11] T.Y. Ma, G.L. Xu, Y. Li, L. Wang, X.M. He, J.M. Zheng, J. Liu, M.H. Engelhard, P. Zapol, L.A. Curtiss, J. Jorne, K. Arnine, Z.H. Chen, Revisiting the corrosion of the aluminum current collector in lithium-ion batteries, J. Phys. Chem. Lett. 8 (2017) 1072–1077.
[12] T.C. Hyams, J. Go, T.M. Devine, Corrosion of aluminum current collectors in high-power lithium-ion batteries for use in hybrid electric vehicles, J. Electrochem. Soc. 154 (2007) C390–C396.
[13] Y. Yamada, C.H. Chiang, K. Sodeyama, J.H. Wang, Y. Tateyama, A. Yamada, Corrosion prevention mechanism of aluminum metal in superconcentrated electrolytes, ChemElectroChem 2 (2015) 1687–1694.
[14] J. Wang, Y. Yamada, K. Sodeyama, C.H. Chiang, Y. Tateyama, A. Yamada, Superconcentrated electrolytes for a high-voltage lithium-ion battery, Nat. Commun. 7 (2016) 12032.
[15] K. Matsumoto, K. Inoue, K. Nakahara, R. Yuge, T. Noguchi, K. Utsugi, Suppression of aluminum corrosion by using high concentration LiTFSI electrolyte, J. Power Sources 231 (2013) 234–238.
[16] D.W. McOwen, D.M. Seo, O. Borodin, J. Vatamanu, P.D. Boyle, W.A. Henderson, Concentrated electrolytes: decrypting electrolyte properties and reassessing Al corrosion mechanisms, Energy Environ. Sci. 7 (2014) 416–426.
[17] X. Tong, F. Zhang, B. Ji, M. Sheng, Y. Tang, Carbon-coated porous aluminum foil anode for high-rate, long-term cycling stability, and high energy density dual-ion batteries, Adv. Mater. 28 (2016) 9979–9985.
[18] T. Li, Carbon-coated aluminum foil as current collector for improving the performance of lithium sulfur batteries, Int. J. Electrochem. Sci. 12 (2017) 3099–3108.
[19] M. Wang, M. Tang, S. Chen, H. Ci, K. Wang, L. Shi, L. Lin, H. Ren, J. Shan, P. Gao, Z. Liu, H. Peng, Graphene-armored aluminum foil with enhanced anticorrosion performance as current collectors for lithium-ion battery, Adv. Mater. 29 (2017) 1703882.
[20] Y. Zhang, W. Wang, P. Li, Y. Fu, X. Ma, A simple solvothermal route to synthesize graphene-modified $LiFePO_4$ cathode for high power lithium ion batteries, J. Power Sources 210 (2012) 47–53.
[21] W.S. Hummers, R.E. Offeman, Preparation of graphitic oxide, J. Am. Chem. Soc. 80 (1958) 1339.
[22] W. Li, X. Geng, Y. Guo, J. Rong, Y. Gong, L. Wu, X. Zhang, P. Li, J. Xu, G. Cheng, M. Sun, L. Liu, Reduced graphene oxide electrically contacted graphene sensor for highly sensitive nitric oxide detection, ACS Nano 5 (2011) 6955–6961.
[23] X.A. Chen, X. Chen, F. Zhang, Z. Yang, S. Huang, One-pot hydrothermal synthesis of reduced graphene oxide/carbon nanotube/α-$Ni(OH)_2$ composites for high performance electrochemical supercapacitor, J. Power Sources 243 (2013) 555–561.
[24] S. Bhaviripudi, X. Jia, M.S. Dresselhaus, J. Kong, Role of kinetic factors in chemical vapor deposition synthesis of uniform large area graphene using copper catalyst, Nano Lett. 10 (2010) 4128–4133.